Structural Characterization and Thermal Conductivity of Type-I Tin Clathrates

G. S. Nolas,*[,†] B. C. Chakoumakos,[‡] B. Mahieu,[§] Gary J. Long,[||] and T. J. R. Weakley[⊥]

R&D Division, Marlow Industries, Inc., 10451 Vista Park Rd., Dallas, Texas 75238; Solid State Division, Oak Ridge National Laboratory, Oak Ridge, Tennessee 37831; Department of Chemistry, University of Louvain, B-1348 Louvain-la-Neuve, Belgium; Department of Chemistry, University of Missouri—Rolla, Rolla, Missouri 65409; and Department of Chemistry, University of Oregon, Eugene, Oregon 97403

Received October 26, 1999. Revised Manuscript Received May 4, 2000

Three tin compounds, Cs_8Sn_{44}, $Cs_8Ga_8Sn_{38}$, and $Cs_8Zn_4Sn_{42}$, representative of the type-I clathrate hydrate crystal structure are structurally characterized by temperature-dependent neutron powder diffraction, 87 K Sn-119 Mössbauer spectroscopy, and room-temperature single-crystal X-ray diffraction. These compounds form in cubic space group $Pm\bar{3}n$ with alkali-metal atoms residing in the polyhedral cavities formed by the tetrahedrally bonded network of Sn atoms. Of particular interest are the atomic displacement parameters (ADPs) exhibited by the alkali-metal atom inside the polyhedral "cages" formed by the framework Sn atoms. The "guest" Cs atoms inside the larger tetrakaidecahedra show a relatively large room-temperature ADP for $Cs_8Ga_8Sn_{38}$ and $Cs_8Zn_4Sn_{42}$; however, in the defect Cs_8Sn_{44} compound this is not the case. This is due to two Sn vacancies in Cs_8Sn_{44} which affect the local symmetry and Sn−Sn bonding. Temperature-dependent ADPs for the defect Cs_8Sn_{44} compound are compared to those for $Cs_8Zn_8Sn_{42}$. These data help elucidate the cause of the different lattice thermal conductivities of these two compounds.

Introduction

There has been considerable interest in Si-clathrates for potential large band-gap semiconductor materials[1] and superconductors.[2] Most recently Ge-clathrates have shown promise for thermoelectric applications.[3−5] These "open-structured" compounds consist of 3D networks of covalent tetrahedrally bonded atoms that form a framework, creating cage-like environments in which "loosely" bonded atoms are enclosed. This arrangement induces interesting transport properties that are directly attributable to this crystal structure.

With few exceptions[6−8] much of the previous work has focused on the Si and Ge derivatives of the clathrate hydrate crystal structure. Herein we report a detailed structural and chemical characterization of representative Sn-clathrate compounds with the type-I hydrate structure. Our aim is to understand the structural characteristics of these materials and how they influence the thermal transport of Sn-clathrates. A careful characterization of the crystal structure and bonding scheme of these compounds will allow a more complete understanding of their transport properties and thus, perhaps, realize their potential as thermoelectric materials. We employ single-crystal X-ray diffraction (XRD), neutron diffraction measurements, and Sn-119 Mössbauer spectroscopy. In addition, the measured atomic displacement parameters (ADPs) from temperature-dependent powder neutron diffraction measurements are used to analyze and correlate the structural data to the low thermal conductivity of these compounds.

Sample Preparation and Experimental Details

Sn-clathrates were prepared in a similar manner as previously reported to provide phase-pure specimens.[3,6,7] High purity elements were mixed in the appropriate stoichiometric proportions in an argon atmosphere glovebox and reacted for 2 weeks at 550 °C inside a tungsten crucible which was itself sealed (welded) inside a stainless steel canister. The canister was evacuated and backfilled with high purity argon gas before sealing. The welded stainless steel canister ensured sample encapsulation even though the vapor pressure of the alkali-

* Corresponding author. E-mail: gnolas@marlow.com.
† Marlow Industries, Inc.
‡ Oak Ridge National Laboratory.
§ University of Louvain.
|| University of Missouri—Rolla.
⊥ University of Oregon.

(1) Demkov, A. A.; Windl, W.; Sankey, O. F. *Phys. Rev. B* **1996**, *53*, 11288−11291, and references therein.
(2) Kawaji, H.; Horie, H.; Yamanaka, S.; Ishikawa, M. *Phys. Rev. Lett.* **1995**, *74*, 1427−1429.
(3) Nolas, G. S. In *Thermoelectric Materials—The Next Generation Materials for Small-Scale Refrigeration and Power Generation Applications*; Tritt, T. M., Mahan, G., Lyon, H. B., Jr., Kanatzidis, M. G., Eds.; Mater. Res. Soc. Symp. Proc.; Mater. Res. Soc.: Pittsburgh, PA, 1999; Vol. 545, pp 435−442.
(4) Nolas, G. S.; Cohn, J. L.; Slack, G. A.; Schujman, S. B. *Appl. Phys. Lett.* **1998**, *73*, 178−180.
(5) Cohn, J. L.; Nolas, G. S.; Fessatidis, V.; Metcalf, T. H.; Slack, G. A. *Phys. Rev. Lett.* **1999**, *82*, 779−782.
(6) Nolas, G. S.; Weakley, T. J. R.; Cohn, J. L. *Chem. Mater.* **1999**, *11*, 2470−2473.
(7) Nolas, G. S.; Cohn, J. L.; Nelson, E. In *Proceedings of the Eighteenth International Conference on Thermoelectrics*, in press.
(8) For an overview of the work on structural properties of Sn-clathrate compounds found in the literature see ref 6, and references therein.

10.1021/cm990686y CCC: $19.00
Published on Web 06/27/2000

Table 1. Single-Crystal XRD of $Cs_8Ga_8Sn_{38}$[a]

space group	$Pm\bar{3}n$
a_o, Å	12.0792(18)
Z	1
T, K	300
calcd density, g/cm^3	5.776
measd density, g/cm^3	5.7
$R(F)$	0.099
$Rw(F)$	0.103
χ^2	3.51
U(Cs1), Å^2	0.012(3)
U(Cs2), Å^2	0.034(5)
U(Sn1), Å^2	0.011(9)
U(Sn2), Å^2	0.016(1)
x(Sn2)	0.1832(1)
U(Sn3), Å^2	0.027(7)
y(Sn3)	0.3142(2)
z(Sn3)	0.1186(2)

[a] Atom positions: Cs1, 2a 0,0,0; Cs2, 6d $^1/_4$, $^1/_2$, 0; Sn1, 6c $^1/_4$, 0, $^1/_2$; Sn2, 16i x, x, x; Sn3, 24k 0, y, z.

metal constituent element was relatively high at 550 °C. The resulting compounds consisted of very small crystals with a shiny, somewhat blackish, metallic luster that were not visibly reactive in air or moisture. In the case of Cs_8Sn_{44}, the synthesis approach resulted in a blackish powder that oxidized to a yellowish color if left in air for several hours. This compound was stored in a nitrogen atmosphere. Most of the small crystals of each compound were ground to fine powder for neutron diffraction measurements and Mössbauer spectroscopy. X-ray diffraction analysis of the powdered specimens revealed type-I clathrate lines with no other impurities. To obtain dense samples for electron-beam microprobe (XMP) analysis and thermal conductivity measurements the specimens were ground to fine powders and hot pressed inside a graphite die at 380 °C and 170 MPa for 2 h in an argon atmosphere. The resulting pellets were better than 90% of theoretical density. Cross-sections of these densified pellets were cut and polished for XMP analysis on individual grains which revealed the stoichiometry of these compound. Normalized to full occupancy of the Cs sites, the stoichiometry of the three compounds are $Cs_{8.0}Sn_{43.3}$, $Cs_{8.0}Ga_{8.0}Sn_{37.7}$, and $Cs_{8.0}Zn_{4.1}Sn_{42.6}$. These values agree well with the expected compositions, within experimental error, and qualitatively with the powder neutron Rietveld refinement results $Cs_{7.4(3)}Sn_{42.7(3)}$ and $Cs_8Zn_{3.5(1.1)}Sn_{42.5(1.1)}$, as will be discussed below.

Single-crystal XRD was carried out on the $Cs_8Ga_8Sn_{38}$ and $Cs_8Zn_4Sn_{42}$ specimens by isolating and investigating single-crystals fragments with an Enraf-Nonius CAD-4 single-crystal diffractometer with graphite-monochromator and Mo K radiation. The Laue symmetry $m3m$ was confirmed by the measurement of potential equivalents for several reflections. The structural refinements confirmed the assignment of the space-group $Pm\bar{3}n$ (no. 223), corresponding to the type-I clathrate structure, on the basis of the systematic absences for all the compounds in this report. Absorption corrections based on azimuthal scans were applied. A SIR92 E-map[9] showed five independent crystallographic positions. The TEXSAN program suite,[10] incorporating complex atomic scattering factors, was used in all calculations.

Details of the single-crystal analysis of $Cs_8Zn_4Sn_{42}$ can be found in ref 6. The initial coordinates from those results were used for the case of $Cs_8Ga_8Sn_{38}$. The occupancy factors for the three independent Sn atoms sites were refined. Attempts to refine with these sites shared between Sn and Ga atoms, the sum of occupancy factors being fixed, were unsatisfactory. Table 1 shows the positions and atomic parameters of $Cs_8Ga_8Sn_{38}$, those for $Cs_8Zn_4Sn_{42}$ are tabulated in ref 6. Our results on $Cs_8Ga_8Sn_{38}$ are in general agreement with those of the more precise ones obtained on larger single crystals by Kröner et al.,[11] in particular that the highest Ga/Sn ratio is at the 6c sites. We are therefore confident that our $Cs_8Ga_8Sn_{38}$ specimen is useful for Mössbauer spectroscopy and thermal conductivity measurements.

Neutron-diffraction data were collected on powdered Cs_8Sn_{44} and $Cs_8Zn_4Sn_{42}$ specimens using the HB-4 high-resolution powder diffractometer at the High-Flux Isotope Reactor (HFIR) at Oak Ridge National Laboratory. Neutrons with a wavelength of 1.5005(1) Å, calibrated with a Si standard, were used, and data were collected between 11° and 135° in 2θ. Each sample was sealed in a vanadium can (9 mm i.d. by 5 cm) with He exchange gas for data collection from 10 to 295 K using a closed-cycle He refrigerator. For these data collections, the detector array was scanned in two segments to overlap up to four detectors in the middle of the pattern. Overlapping detectors for a given step serves to average the counting efficiency and the 2θ zero-point shift for each detector. Input for the Rietveld refinement program was prepared by interpolating a constant step-size data set from the raw data. The data were also corrected for the variation in detector counting efficiencies, which were determined using a vanadium standard. Structure refinements were made by the Rietveld method using the GSAS software.[12] The background was defined by a cosine Fourier series with four terms. The coherent scattering lengths used were Cs (5.42 fm), Sn (6.225 fm), and Zn (5.68 fm).[13]

For tin Mössbauer measurements the powdered specimens were mixed with boron nitride powder to ensure an adequate absorber thickness. The Sn-119 Mössbauer spectra were obtained at room temperature and 87 K on a constant-acceleration spectrometer which was calibrated at room temperature with a rhodium matrix Co-57 source and α-iron foil. The Sn-119 spectra were obtained with a room-temperature Sn-119 source in a $CaSnO_3$ matrix, and the isomer shifts are reported relative to $CaSnO_3$. The absorber thicknesses were $\sim$7 mg/cm^2. The spectra have all been fit with one symmetric quadrupole doublet and two singlets as discussed below. The resulting weighted average isomer shifts and quadrupole splittings are valid to ca. ±0.05 mm/s and the relative values are valid to ca. ±0.02 mm/s.

Results and Discussion

In the type-I hydrate crystal structure, the Sn framework atoms form bonds to each other in a distorted tetrahedral arrangement (from heretofore we assume that the Ga or Zn is in the three Sn crystallographic sites where appropriate). These framework atoms form polyhedra with shared faces. Eight polyhedra per cubic unit cell comprise the type-I clathrate structure, two Sn_{20} dodecahedra and six Sn_{24} tetrakaidecahedra. The alkali-metal atoms reside inside these polyhedra, at the 2a and 6b crystallographic positions, respectively. Because of this encapsulation of the alkali-metal atoms the Sn-clathrate compounds are relatively stable in air and moisture, as compared to CsSn for example; the Cs_8Sn_{44} compound, however, will oxidize if not kept in an oxygen and moisture free environment.[6,8] Figure 1 shows the dodecahedron and tetrakaidecahedron that form the type I clathrate structure.

Initially the site occupancies for the 300 K data were allowed to vary in the Rietveld refinements. Those sites which showed significant deficiencies were allowed to

(9) Altomare, A.; Cacarano, G.; Giacovazzo, C.; Guagliardi, A.; Burla, M. C.; Polidori, G.; Camalli, N. J. *Appl. Crystallogr.* **1994**, *27*, 435.

(10) *TeXsan Software for Single-Crystal Structure Analysis*, version 1.7; Molecular Structures Corporation: The Woodlands, TX 77381.

(11) Kröner, R.; Peters, K.; von Schnering, H. G.; Nesper, R. *Z. Kristallogr.* **1998**, *213* 673−674.

(12) Larson, A. C.; Von Dreele, R. B. *Los Alamos National Laboratory Rep.* **1986**, Laur 86−748.

(13) Sears, V. F. *Neutron News* **1992**, 26−37.

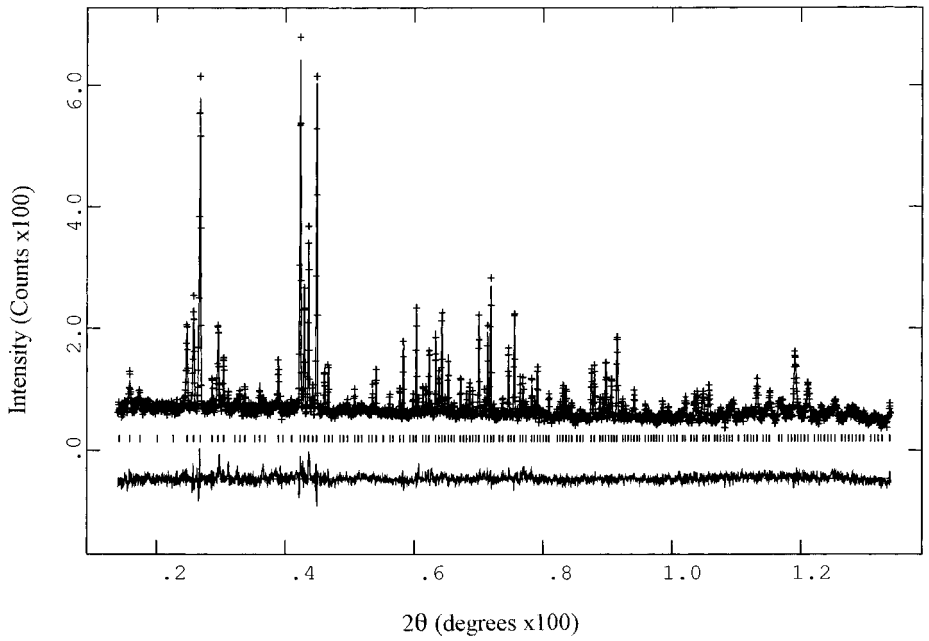

Figure 1. Rietveld profile of room-temperature neutron diffraction data of $Cs_8Zn_4Sn_{42}$. The solid line is the fit to the experimental data, shown as plus marks (+). The tick marks represent the calculated reflection positions and the lower line the difference spectrum.

vary in subsequent refinements, and those that did not, were fixed at full occupation. To assess the precision, accuracy, and degree of parameter correlation involving these occupancies, for each temperature the site occupancies were allowed to vary, even though physically we would not expect these to have any temperature dependence below 300 K. The scatter in some of the site occupancies determined in this manner exceeds the estimated standard deviation from the Rietveld refinement, and thus may provide a more realistic estimate of the uncertainty when the errors returned by the Rietveld refinement method are well-known to be overly precise. The scatter in these occupancies must reflect the data quality, because ideally each temperature should independently provide the same composition.

The Rietveld results for Cs_8Sn_{44} indicate that the Cs site at the 2a position is fully occupied, the Cs site at the 6d position is 90(5)% occupied, the Sn site at the 6c position 71(8)% occupied, the Sn site at the 16i position is 90(2)% occupied, and the Sn site at the 24k position is fully occupied. This yields a composition of $Cs_{7.4(3)}Sn_{42.7(3)}$. Some weak impurity lines were observed corresponding to unreacted tin and Cs compounds. The Rietveld results for $Cs_8Zn_4Sn_{42}$ indicate that the Cs sites at the 2a position and the 6d position are fully occupied, the Zn content of the Sn(1) site at the 6c position is 58(19)%, and the Sn sites at the 16i position and the 24k position are fully occupied by Sn. This yields a composition of $Cs_8Zn_{3.5(1.1)}Sn_{42.5(1.1)}$. No impurity lines were observed in this compound. Figure 2 shows the Rietveld results of room-temperature neutron diffraction on $Cs_8Zn_4Sn_{42}$. Table 2 contains the Sn bond lengths and angles obtained from Rietveld refinements from powder neutron diffraction and single-crystal XRD data. Also tabulated are XRD results for powdered Cs_8Sn_{46} from Grin' et al.[14] and single-crystal $K_{1.6}Cs_{6.4}Sn_{44}$ from

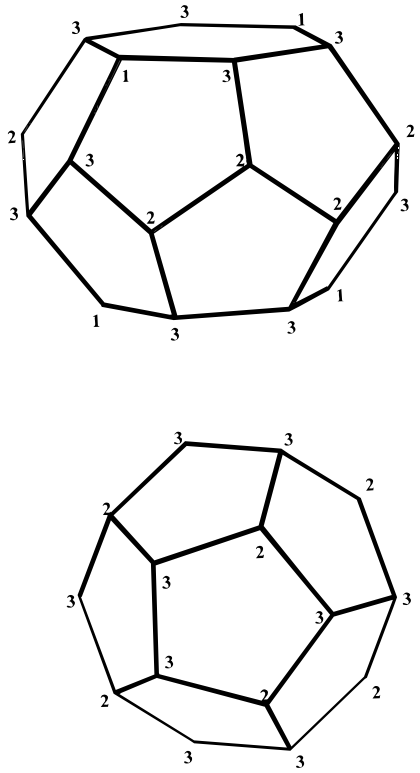

Figure 2. Schematic of the dodecahedron (bottom) and tetrakaidecahedron (top) in the type-I clathrate structure. The three crystallographic sites 6c, 16i, and 24k are numbered 1, 2, and 3, respectively.

Zhao and Corbett.[15] The room-temperature isotropic ADPs(described below), bond lengths and angles for the Cs_8Sn_{44} compound reported here are in excellent agreement with those from a single-crystal X-ray study of $K_{1.6}Cs_{6.4}Sn_{44}$,[15] but are in poor agreement with those from a powder X-ray study of purported Cs_8Sn_{46}.[14] In

(14) Grin', Y. N.; Melekhov, L. Z.; Chutonov, K. A.; Yatsenko, S. P. *Sov. Phys. Crystallogr.* **1987**, *32*, 290−291.

(15) Zhao, J.-T.; Corbett, J. D. *Inorg. Chem.* **1994**, *33*, 5721−5726.

Table 2. Interatomic Bond Lengths (Å) and Bond Angles (deg) of Type-I Sn-clathrate Compounds from Single-Crystal XRD Data (denoted by an asterisk) and Neutron Powder Data (Cs_8Sn_{44} and $Cs_8Zn_4Sn_{42}$)[a]

	$Cs_8Ga_8Sn_{38}$*	$Cs_8Zn_4Sn_{42}$	$Cs_8Zn_4Sn_{42}$*	Cs_8Sn_{44}	$K_{1.6}Cs_{6.4}Sn_{44}$*	Cs_8Sn_{46}
			Bond Lengths			
Cs1−Sn2	3.833(2)	3.848(3)	3.844(2)	3.841(6)	3.827(3)	3.775
Cs1−Sn3	4.056(3)	4.071(3)	4.073(2)	4.113(7)	4.086(4)	4.113
Cs2−Sn1i	4.2706(3)	4.2869(1)	4.2860(3)	4.2799(1)	4.2725(3)	4.277
Cs2−Sn2	4.4936(7)	4.510(1)	4.5104(6)	4.503(2)	4.4977(9)	4.520
Cs2−Sn3	4.026(2)	4.045(2)	4.041(1)	4.009(4)	4.015(2)	4.054
Sn1−Sn3i	2.750(3)	2.758(3)	2.757(2)	2.712(7)	2.724(4)	2.686
Sn2−Sn2ii	2.796(5)	2.805(7)	2.810(4)	2.802(12)	2.8411(5)	2.925
Sn2−Sn3	2.830(2)	2.837(2)	2.840(1)	2.863(4)	2.843(2)	2.806
Sn3−Sn3iii	2.864(5)	2.890(6)	2.880(4)	2.880(13)	2.881(6)	3.048
			Bond Angles			
Sn3−Sn1−Sn3[b]	109.48(5)	109.32(6)	109.45(4)	110.0(1)	109.7	108.2
Sn3−Sn1−Sn3[c]	109.46(9)	109.7(1)	109.51(7)	108.4(2)	109.1	112.1
Sn3−Sn2−Sn3	106.73(7)	106.72(9)	106.64(5)	105.9(2)	106.1	104.2
Sn3−Sn2−Sn3	112.06(6)	112.08(8)	112.15(4)	112.7(1)	112.6	114.2
Sn1−Sn3−Sn2	107.29(8)	107.4(1)	107.40(6)	107.7(2)	107.7	110.8
Sn1−Sn3−Sn3	125.27(5)	125.11(6)	102.25(4)	125.8(9)	125.5	123.9
Sn2−Sn3−Sn2	102.87(9)	103.0(1)	102.82(7)	101.5(2)	102.0	101.9
Sn2−Sn3−Sn3	106.01(6)	105.89(7)	105.94(4)	105.7(2)	105.7	103.5

[a] Data for purported Cs_8Sn_{46} are from Grin' et al.[14] and for $K_{1.6}Cs_{6.4}Sn_{44}$ from Zhao and Corbett.[15] Symmetry code: (i) z, y, z; (ii) $^1/_2 - x, ^1/_2 - z, ^1/_2 - y$, (iii) $-x, y, -z$. [b] Pentagonal face of tetrakaidecahedron;. [c] Hexagonal face of tetrakaidecahedron (see Figure 1).

the latter case we believe systematic errors in the X-ray study account for the large discrepancies. In the case of the $Cs_8Zn_4Sn_{42}$, the Rietveld refined neutron diffraction data is in excellent agreement with that obtained from single-crystal XRD data.[6]

The Sn−Sn−Sn bond angles range from 102 to 126° and the Sn−Sn bond lengths are comparable to those of diamond structured α-Sn at 2.810 Å,[16] as shown in Table 2. The bond lengths and angles of Cs_8Sn_{44} are slightly larger than those of the other Sn-clathrates. This is due to the two vacancies per unit cell randomly distributed on the 6c crystallographic sites, and results in a distortion of the local symmetry surrounding these vacancies therefore changing the Sn−Sn bonds. This is also corroborated by the large ADPs of the 24k site as well as our Mössbauer spectral results.

The Sn-119 Mössbauer spectra of the three representative samples prepared for this report, along with a $Rb_8Ga_8Sn_{38}$ compound, have been measured at 87 K. The spectra are all similar to that of $Cs_8Zn_4Sn_{42}$ shown in Figure 3. From preliminary fits it was obvious that the spectra could not be fit with a single doublet although they could be fit adequately with a symmetric doublet and a singlet. In view of the three crystallographically different Sn sites (6c, 16i, and 24k) in these compounds, it was decided to fit the spectra with three components constrained to have the same relative areas as the tin occupancy of each of these crystallographic sites.

Again from preliminary fits, it was obvious that two of these sites, the 6c and 16i sites, require only singlets which have essentially the same isomer shifts. As a consequence, all the spectra were fit with singlets for the 6c and 16i sites and a symmetric quadrupole doublet for the 24k site. The resulting fits, although far from unique, do clearly indicate that the 24k site must have a substantial quadrupole splitting. This splitting is expected because of the extensive distortion of this site from cubic symmetry. Our structural results indicate that for $Cs_8Zn_4Sn_{42}$, the Zn atoms are randomly distributed on the 6c crystallographic site and thus the three spectral components were constrained to be in the ratio of 2:16:24. Similarly, for Cs_8Sn_{44}, the two Sn vacancies occur randomly only on the 6c site and thus the three spectral components were constrained to be in the ratio of 4:16:24. In $Cs_8Ga_8Sn_{38}$, the Ga atoms occupy all three of the Sn sites and thus the three spectral components were constrained to be in the ratio of 6:16:24. This is also assumed to be the case for $Rb_8Ga_8Sn_{38}$. The hyperfine parameters corresponding to these fits are given in Table 3 along with results for α-Sn and β-Sn for comparison.

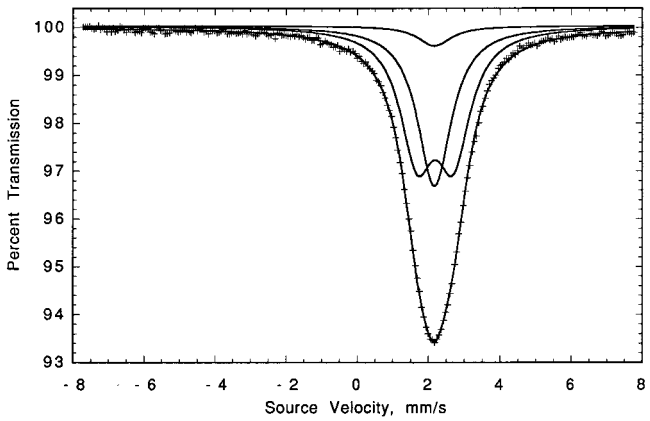

Figure 3. Sn-119 Mössbauer spectrum of $Cs_8Zn_4Sn_{42}$. The experimental data are given by the + symbols and the four solid lines represent the 6c, 16i, and 24k site spectral components and the total fit, the parameters of which are given in Table 3.

The hyperfine parameters of the four samples studied herein are rather similar, as would be expected from the similarity of the bonding in the four compounds. However, real differences in the quadrupole splittings are observed for the 24k site. Specifically, the quadrupole splitting of the 24k site in Cs_8Sn_{44} is larger than in the remaining three compounds. As might be expected, the Sn vacancies on the 6c site in Cs_8Sn_{44} lower the 24k site electronic symmetry more than does the presence of Zn on the 6c site in $Cs_8Zn_4Sn_{42}$ or Ga on the three framework sites (6c, 16i, and 24k) in Cs_8Ga_8-

(16) Goyunova, N. A. in *The Chemistry of Diamond-like Semiconductors*; MIT Press: Cambridge, MA, 1965.

Table 3. The 87 K Sn-119 Mössbauer Spectral Hyperfine Parameters[a]

sample	site	δ (mm/s)	ΔE_Q (mm/s)	Γ (mm/s)	relative area (%)
$Rb_8Ga_8Sn_{38}$	6c	2.12	0.00	1.08	6
	16i	2.12	0.00	1.08	16
	24k	2.11	0.80	1.08	24
	wt av	2.11	0.52	1.08	
$Cs_8Ga_8Sn_{38}$	6c	2.18	0.00	1.07	6
	16i	2.18	0.00	1.07	16
	24k	2.17	0.96	1.07	24
	wt av	2.17	0.58	1.07	
$Cs_8Zn_4Sn_{42}$	6c	2.15	0.00	1.13	2
	16i	2.15	0.00	1.13	16
	24k	2.16	1.01	1.13	24
	wt av	2.16	0.58	1.13	
Cs_8Sn_{44}	6c	2.28	0.00	1.38	4
	16i	2.28	0.00	1.38	16
	24k	2.33	1.22	1.38	24
	wt av	2.30	0.66	1.38	
α-Sn		2.03	0.00	1.00	
β-Sn		2.63	0.55	1.35	

[a] The isomer shifts are given relative to $CaSnO_3$. Data for α-Sn and β-Sn are from the literature (see text).

Sn_{38} and $Rb_8Ga_8Sn_{38}$. As shown in Table 2, this is also apparent from the neutron diffraction and single-crystal XRD data.

The weighted average isomer shifts are all lower than the 80 K value of 2.63 mm/s reported for β-Sn[17] and much closer to that of α-Sn. The 87 K value of 2.16 mm/s found herein is representative of covalent bonding and eliminates the possibility of the compounds containing Sn(II) and Sn(IV). The isomer shifts indicate that the s-electronic density at the Sn-119 nucleus corresponds to ~1.05 s electrons per atom, a value which is in good agreement with the close-to-tetrahedral tin bonding. A further argument supporting the covalent nature of the bonding is provided by the variation of the resonant absorption area as a function of temperature. From measurements at 295 and 87 K for $Cs_8Zn_4Sn_{42}$, for example, a slope of $-0.002\,26\ K^{-1}$ was obtained for ln(relative area) vs T. This value is typical of strongly bonded covalent compounds and is far lower than the values found for molecular compounds.[18]

The specific framework and thermal parameters are an important aspect of this structure. One of the more interesting structural features is the anisotropy and large thermal motion of the alkali-metal in the Sn_{24} polyhedra. These properties drastically affect the thermal transport in these compounds. Rietveld-refined neutron diffraction data for $Cs_8Zn_4Sn_{42}$ and Cs_8Sn_{44} are tabulated in Tables 4 and 5, respectively. In the case of $Cs_8Zn_4Sn_{42}$ the temperature-dependent isotropic ADPs, $U(T)$, of Cs in the dodecahedra, 2a, or Cs1 site, and those of the three Sn sites are similar in magnitude. That of the Cs in the tetrakaidecahedra, 6d, or Cs2 site, is much larger, as is shown in Figure 4 and Table 4. The temperature-dependent ADP data for Cs2 indicates that most of the disorder in this site is likely due to the "rattling", or dynamic, motion of the Cs atom. The framework Sn atoms show a minimal temperature dependence which indicates a relatively stiff framework.

(17) Flinn, P. A. In *Mössbauer Isomer Shifts*; Shenoy, G. K., Wagner, F. E., Eds., North-Holland Pub. Co.: Amsterdam, 1978; p 593.

(18) Parish, R. V. In *Mössbauer Spectroscopy Applied to Inorganic Chemistry*; Long, G. J., Ed.; Plenum Press: New York, 1984; p 549.

Table 4. Rietveld Refinement Results for $Cs_8Zn_4Sn_{42}$, $Pm\bar{3}n$, $Z = 1$, from Neutron Powder Diffraction Data

T, K	11	60	120
a_0, Å	12.0928(2)	12.0951(2)	12.1014(2)
calcd density, g/cm^3	5. 954	5. 597	6.086
$R(F)$	0.0637	0.0635	0.0626
$Rw(F)$	0.0805	0.0794	0.0761
χ^2	1.469	1.429	1.304
U(Cs1), Å^2	0.003(2)	0.003(2)	0.007(2)
U(Cs2), Å^2	0.006(1)	0.010(1)	0.019(1)
U(Sn1), Å^2	0.002(2)	0.004(2)	0.008(2)
Zn:Sn (Sn1)	0.4:0.6(2)	0.5:0.5(2)	0.9:0.1(2)
U(Sn2), Å^2	0.0028(5)	0.004(2)	0.0053(5)
x(Sn2)	0.1833(2)	0.1831(2)	0.1831(2)
U(Sn3), Å^2	0.0048(5)	0.0052(5)	0.0078(5)
y(Sn3)	0.3139(1)	0.3138(2)	0.3141(2)
z(Sn3)	0.1190(2)	0.1188(2)	0.1187(2)
T, K	180	240	300
a_0, Å	12.1094(2)	12.1175(2)	12.1252(2)
calcd density, g/cm^3	5. 918	6.005	5.951
$R(F)$	0.0644	0.0624	0.0646
$Rw(F)$	0.0787	0.0767	0.0777
χ^2	1.386	1.317	1.348
U(Cs1), Å^2	0.009(2)	0.017(2)	0.016(2)
U(Cs2), Å^2	0.023(2)	0.032(2)	0.035(2)
U(Sn1), Å^2	0.010(2)	0.013(2)	0.015(2)
Zn:Sn (Sn1)	0.4:0.6(2)	0.7:0.3(2)	0.6:0.4(3)
U(Sn2), Å^2	0.0086(6)	0.0096(6)	0.0123(6)
x(Sn2)	0.1831(1)	0.1831(1)	0.1832(2)
U(Sn3), Å^2	0.0101(6)	0.0119(6)	0.015(2)
y(Sn3)	0.3140(2)	0.3140(2)	0.3139(2)
z(Sn3)	0.1188(2)	0.1187(2)	0.1191(2)

[a] Atom positions: Cs, 2a 0, 0, 0; Cs2, 6d $^1/_4$, $^1/_2$, 0; Sn1, 6c $^1/_4$, 0, $^1/_2$; Sn2, 16i x, x, x; Sn3, 24k 0, y, z.

Table 5. Rietveld Refinement Results for Cs_8Sn_{44}, $Pm\bar{3}n$, $Z = 1$, from Neutron Powder Diffraction Data

T, K	11	60	120
a_0, Å	12.0728(4)	12.0748(4)	12.0808(4)
calcd density, g/cm^3	5. 703	5. 596	5. 6718
$R(F)$	0.0766	0.0748	0.0723
$Rw(F)$	0.0960	0.0924	0.0916
χ^2	1.944	1.798	1.757
U(Cs1), Å^2	0.010(3)	0.008(3)	0.013(4)
U(Cs2), Å^2	0.000(4)	0.000(4)	0.020(5)
n(Cs2)	0.91(5)	0.85(5)	0.97(5)
U(Sn1), Å^2	0.005(5)	0.011(5)	0.003(5)
n(Sn1)	0.66(5)	0.87(3)	0.64(4)
U(Sn2), Å^2	0.005(2)	0.004(2)	0.007(2)
n(Sn2)	0.91(3)	0.87(3)	0.91(3)
x(Sn2)	0.1829(2)	0.1831(2)	0.1831(2)
U(Sn3), Å^2	0.032(2)	0.034(2)	0.035(2)
y(Sn3)	0.3175(5)	0.3184(5)	0.3176(5)
z(Sn3)	0.1186(5)	0.1190(5)	0.1182(5)
T, K	180	240	300
a_0, Å	12.0897(4)	12.0980(4)	12.1054(4)
calcd density, g/cm^3	5. 637	5. 680	5.653
$R(F)$	0.0679	0.0671	0.0661
$Rw(F)$	0.0847	0.0829	0.0825
χ^2	1.501	1.437	1.419
U(Cs1), Å^2	0.013(3)	0.012(1)	0.024(7)
U(Cs2), Å^2	0.014(5)	0.023(5)	0.024(5)
n(Cs2)	0.85(4)	0.89(5)	0.91(5)
U(Sn1), Å^2	0.017(5)	0.021(6)	0.015(5)
n(Sn1)	0.72(3)	0.70(4)	0.67(4)
U(Sn2), Å^2	0.010(2)	0.014(2)	0.012(1)
n(Sn2)	0.89(3)	0.92(3)	0.90(2)
x(Sn2)	0.1832(2)	0.1829(3)	0.1832(3)
U(Sn3), Å^2	0.036(2)	0.038(2)	0.039(2)
y(Sn3)	0.3185(5)	0.3175(5)	0.3183(5)
z(Sn3)	0.1190(5)	0.1191(5)	0.1189(6)

[a] Atom positions: Cs, 2a 0,0,0; Cs2, 6d $^1/_4$, $^1/_2$, 0; Sn1, 6c $^1/_4$, 0, $^1/_2$; Sn2, 16i x, x, x; Sn3, 24k 0, y, z.

This is consistent with a model whereby the Cs atoms "rattle" about in the relatively large tetrakaidecahedra "cage". This is in contrast with the data for Cs_8Sn_{44}, as

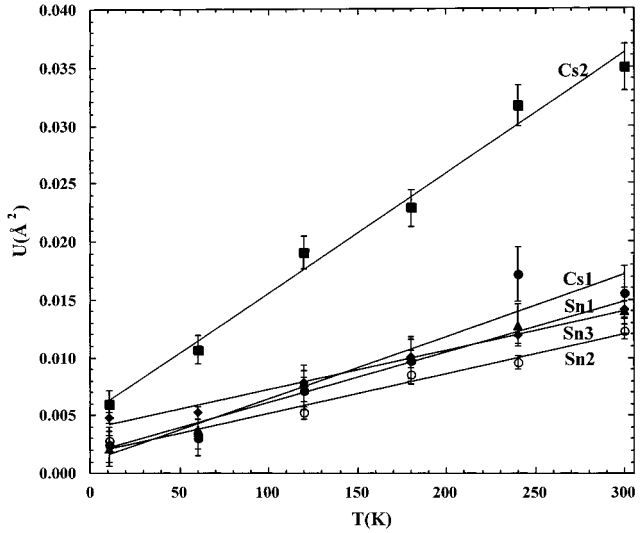

Figure 4. Temperature dependence of the isotropic ADPs for $Cs_8Zn_4Sn_{42}$. The apparent $U(T)$ is large for Cs2 as compared to the other constituent elements.

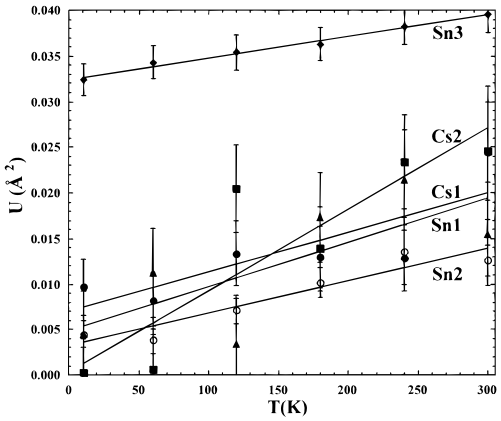

Figure 5. Lattice thermal conductivity versus temperature for three polycrystalline Sn-clathrates.

shown in Figure 5 and Table 5. Although the ADPs are generally similar for the Cs2 site as in the Cs1 site, the largest ADPs occur for Sn in the 24k or Sn3 site. In addition, there is little temperature dependence to $U(T)$ for Sn3. This implies a distortion, i.e., positional disorder, of this site created by the Sn vacancies on the 6c site, as corroborated by the Mössbauer spectral data. Apparently in the defect type-I structure of Cs_8Sn_{44} the positional disorder of the framework atoms ruins the rigidity of the polyhedra.

Recently[19] it has been shown that ADPs can be used to determine characteristic localized vibration frequencies for weakly bound atoms that "rattle" within their atomic "cages". This approach, which assumes the "rattling" atoms act as harmonic oscillators, has been successfully applied to compounds with the skutterudite crystal structure[19] and Ge-clathrates,[19−21] as well as

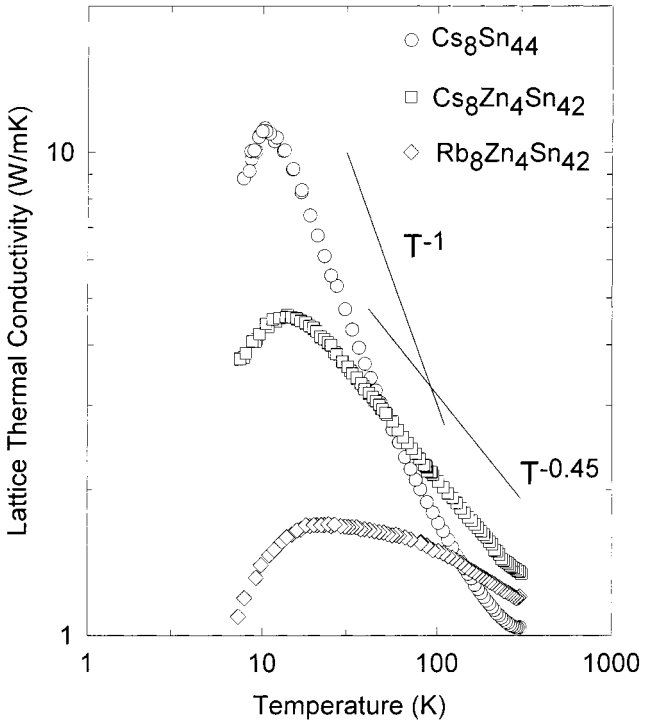

Figure 6. Temperature dependence of the isotropic ADPs for Cs_8Sn_{44}. The $U(T)$ for Cs2 is comparable to the other constituent elements. The largest $U(T)$ is observed for Sn3. The weak temperature dependence indicates that the relatively large $U(T)$ is most likely due to static disorder induced by the two vacancies per unit cell on the Sn1 site.

others compounds.[19] The localized vibration of the "rattler" atom can be described by an Einstein oscillator model such that $U(T) = k_BT/m(2\pi\nu)^2$ where $U(T)$ is the slope of the isotropic mean-square displacement, k_B is the Boltzmann constant, m is the mass of the "rattling" atoms under the assumption that their "cages" are relatively rigid and the frequency of vibration. The ADP data then can be used to estimate the "Einstein temperature" of these atoms ($T_E = h/k_B$) where h is Planck's constant and, more importantly, the lattice contribution to the thermal conductivity, κ_L, for compounds in which at least one of the constituents is weakly bound and therefore "rattles" about in an oversized cage, i.e., clathrate-like compounds.[19,20,21] Using this approach we estimate $T_E = 61$ K and $\kappa_L = 0.7$ W/mK for $Cs_8Zn_4Sn_{42}$. This is only about half of the measured room-temperature value of $\kappa_L = 1.3$ W/mK.[6] This is an indication that "rattle"-type phonon scattering may not be the predominant phonon scattering mechanism in $Cs_8Zn_4Sn_{42}$. In the case of Cs_8Sn_{44} this type of an analysis is not appropriate since $U(T)$ for Cs2 is similar to that of the other constituent atoms (Figure 5). That is, the Cs2 atoms do not "rattle" about as readily due to the distortion created by the Sn vacancies.

Figure 6 shows κ_L of polycrystalline Cs_8Sn_{44} and $Cs_8Zn_4Sn_{42}$ as well as for $Rb_8Zn_4Sn_{42}$.[5−7] The thermal conductivity of $Cs_8Ga_8Sn_{38}$ has a similar temperature dependence as $Cs_8Zn_4Sn_{42}$ and is therefore not shown in the figure. Cs_8Sn_{44} exhibits a $1/T$ temperature dependence typical of simple crystalline insulators dominated by phonon−phonon scattering. The low κ_L

(19) Sales, B. C.; Chakoumakos, B. C.; Mandrus, D.; Sharp, J. W.; Dilley N. R.; Maple, M. B. In *Thermoelectric Materials—The Next Generation Materials for Small-Scale Refrigeration and Power Generation Applications*; Tritt, T. M., Mahan, G., Lyon, H. B., Jr., Kanatzidis, M. G., Eds.; Mater. Res. Soc. Symp. Proc.; Mater. Res. Soc.: Pittsburgh, PA, 1999; Vol. 545, pp 13−18. Sales, B. C.; Chakoumakos, B. C.; Mandrus, D.; Sharp J. W. *J. Solid State Chem.* **1999**, *146*, 528−532.

(20) Nolas, G. S.; Weakley, T. J. R.; Cohn, J. L.; Sharm, R. *Phys. Rev. B* **2000**, *61*, 3845−3850 2000.

(21) Chakoumakos, B. C.; Sales, B. C.; Mandrus, D. C.; Nolas, G. S. *J. Alloys Compd.* **1999**, *296*, 80−86.

values may be due to the complex crystal structure, i.e., 56 atoms per unit cell, in this compound.[22] In the case of the $Cs_8Zn_4Sn_{42}$ specimen κ_L also increases with decreasing temperature however not as strongly, with a $T^{-0.45}$ dependence, typical of mass-fluctuation disorder scattering of the phonons. It may be that the "rattle" vibrational modes of Cs2 in this compound are not within the range of the acoustic phonons. It would therefore not be possible for the "rattling" to couple to the framework phonon modes. The additional bonding induced between the Cs and Sn atoms neighboring the vacancies in Cs_8Sn_{44} apparently constrain the Cs2 displacements (see Figure 5). This structural difference between $Cs_8Zn_4Sn_{42}$ and Cs_8Sn_{44}, therefore, appears to be the source of their differing thermal conductivities. The localized vibrations of Cs2 in $Cs_8Zn_4Sn_{42}$ may, however, couple to the optic phonons producing resonant damping of these phonons. In the case of $Rb_8Zn_4Sn_{42}$ the Rb atoms are smaller than the Cs atoms and therefore are more free to "rattle" inside the polyhedra formed by the (Zn,Sn) atoms. These localized vibrations may provide a more prominent phonon scattering affect in this compound, as indicated by the temperature dependence of κ_L for $Rb_8Zn_4Sn_{42}$ (see Figure 6). While the enhanced thermal motion of the Cs2 and Rb2 atoms in these Sn-clathrates appear to diminish κ_L, the effect is not as great as that caused by the Sr2 motion in $Sr_8Ga_{16}Ge_{30}$[20,21] where the Sr vibration frequencies lie in the range of the acoustic phonons. In addition, the $Sr_8Ga_{16}Ge_{30}$ compound possesses static as well as dynamic disorder on the Sr2 site thereby resulting in a "glasslike" temperature-dependent thermal conductivity.[3−5,20,21]

(22) Slack, G. A. In *Solid State Physics*; Ehrenreich, H., Seitz, F., Turnbull, D., Eds.; Academic Press: New York, 1979; Vol. 34, pp 1−71.

Conclusion

The synthesis, structural analysis, and bonding between Sn atoms of three representative compounds with the type-I clathrate structure have been reported. The temperature dependence of the atomic displacement parameters of Cs atoms in the tetrakeidekahedra of $Cs_8Zn_4Sn_{42}$ imply a "rattling" motion of these atoms as compared to the Sn framework. In the case of Cs_8Sn_{44}, however, the Sn vacancies create a distortion in the Sn3 sites thereby effectively eliminating the "rattling" motion of the Cs2 atoms. The result is that the temperature dependence of the thermal conductivity of Cs_8Sn_{44} is typical of crystalline solids. The low thermal conductivity, along with the semiconductor behavior displayed by these compounds, illustrates why these compounds are of growing interest for potential thermoelectric applications.

Acknowledgment. G.S.N. acknowledges the support of the U.S. Army Research Laboratory under contract number DAAD17-99-C-006. Oak Ridge National Laboratory is managed by Lockheed Martin Energy Research Corporation for the U.S. Department of Energy under contract number DE-AC05-96OR22464. G.J.L. acknowledges the support of the Division of Materials Research of the U.S. National Science Foundation for grant DMR-9521739.

CM990686Y